

Stress overshoot and configuration-induced hysteresis in type-II superconducting films with a periodic pinning array

Q. H. Chen,^{1,*} C. Carballeira,² T. Nishio,¹ B. Y. Zhu,³ and V. V. Moshchalkov¹

¹*Institute for Nanoscale Physics and Chemistry (INPAC), Nanoscale Superconductivity and Magnetism Group, K. U. Leuven, Celestijnenlaan 200 D, 3001 Leuven, Belgium*

²*LBTS, Departamento de Física da Materia Condensada, Universidade de Santiago de Compostela, Santiago de Compostela E-15782, Spain*

³*National Laboratory for Superconductivity, Institute of Physics, Beijing National Laboratory for Condensed Matter Physics, Chinese Academy of Sciences, Beijing 100190, China*

(Received 1 August 2008; revised manuscript received 31 October 2008; published 25 November 2008)

We have simulated numerically the voltage-current (V - I) characteristics of a type-II superconducting film with three different types of periodic magnetic dot arrays. Our findings show that, in the absence of thermal fluctuations, the vortex-vortex and pin interactions vary with the configuration of the dot array. Subsequently, the three systems present different degrees of stress overshoot that give rise to different hysteresis and types of transitions in their V - I curves. The width of the hysteresis can be analytically estimated by using an infinite-range model, which is in good agreement with the simulations.

DOI: 10.1103/PhysRevB.78.172507

PACS number(s): 74.25.Qt, 68.35.Rh, 74.25.Fy, 74.90.+n

I. INTRODUCTION

Hysteresis that represents the history dependence of a system happens in a number of physical systems. For instance, in a type-II superconducting (SC) system with a *random* pinning array, both experimental and theoretical data have shown that there exists hysteresis along with first-order transitions in the curve of the average velocity (\bar{v}) versus the driving force (F_d) (Ref. 1), which corresponds to the macroscopically measured voltage-current (V - I) characteristics.¹ The appearance of this phenomenon is greatly dependent on the vortex-vortex interaction, vortex density, pinning center density, pinning strength, and thermal fluctuations. Recently, the increasing attention to the physics of type-II superconducting films with a *periodic* pinning array (PPA) (Refs. 2–6) has also attracted the interest of researchers to the behavior of the V - I curves in these systems. In particular, Reichhardt *et al.*⁴ have shown that, in the absence of thermal fluctuations, the transition between the pinned and the plastic flow phase of a superconducting film with a PPA is of the first order and it is accompanied by a hysteresis when the number of vortices, N_v , is greater than the number of pinning sites, N_p . The authors ascribed this interesting phenomenon to different regimes of plastic flows: one-dimensional (1D) interstitial flow of vortices between the rows of pinning sites, two-dimensional (2D) pin-to-pin and winding interstitial motion of vortices, and 1D incommensurate flow. However, not only very weak hysteresis occurs at the *main transition*, i.e., a transition from the plastic flow to the moving phase, and the curve remains continuous at this regime.⁴ Zhu *et al.*⁵ demonstrated that even in a superconducting film with a triangular pinning array, this phenomenon can be also observed at zero temperature under relatively *weak* vortex-vortex interaction condition.

The behavior of the V - I characteristics of a superconducting film with a PPA can be understood in terms of a competition of vortex-vortex and vortex-pin interactions, which may lead the system to disorder. In this work we argue that this disorder may cause dynamic *stress overshoot*.⁷ In a sys-

tem with a random pinning array or with a PPA at the incommensurate field, the V - I curve clearly appears as discontinuous and perhaps with hysteresis when the magnitude of this stress overshoot, M , is larger than its critical value, M_c (Ref. 7). However, in the case with a PPA at the commensurate field the moving vortex lattice remains phase-locked if the vortex-vortex interaction is strong enough, leading to $M \leq M_c$. This gives rise to a continuous velocity change at the main transition without hysteresis. In contrast, for a weak vortex-vortex interaction the situation with $M > M_c$ will still be possible.

After studies by Reichhardt *et al.*⁴ and Zhu *et al.*⁵ several key issues have been formulated: in the absence of thermal fluctuations, can we obtain the hysteresis along with the first-order transitions in a SC system with a PPA when the pinning is relatively strong? Can we also observe it at the main transition both under commensurate and incommensurate conditions? Is it controllable? Motivated by these challenges, we have employed intensive numerical simulations and found that the *configuration of the pinning site array* plays an important role in the appearance and control of the hysteresis at the first-order transition in these systems. To probe these ideas, we have numerically simulated the V - I characteristics in absence of thermal fluctuations of a type-II superconducting film with three different periodic pinning arrays, namely, a square ferromagnetic (SFM) dot array, a triangular ferromagnetic (TFM) dot array, and an antiferromagnetic (AFM) dot array.⁶ To maximize the main configuration-induced hysteresis and skip the subtle effects induced by interstitial vortices⁴ we have focused our investigations on the first matching field, H_1 (i.e., the field at which $N_v = N_p$). The so-obtained V - I curves present, in some cases, a significant and intrinsic hysteresis, together with continuous or discontinuous jumps or drops at the main transition; a behavior that may be interpreted with the help of snapshots of the system and of the vortex trajectories. The width of the hysteresis resulting from these simulations is in good agreement with the one that can be analytically estimated in the framework of an infinite-range model.⁷ Our results clearly show that the

appearance of the hysteretic first-order transition and the width of the hysteresis can be easily controlled by just tuning the configuration of the PPA. In order to highlight this interesting phenomenon we identify it as *configuration-induced hysteresis*.

II. MODEL

We model the two-dimensional superconducting system with periodic boundary conditions in the x and y directions assuming that the motion of vortices is *overdamped*. The total force acting on vortex i is then governed by $\vec{F}_i = \vec{F}_d + \vec{F}_i^{vv} + \vec{F}_i^{vp} = \eta \vec{v}_i$ (Ref. 8), where η is the viscosity coefficient (taken to be unity), $\vec{F}_i^{vv} = \sum_{j=1}^{N_v} f_0 K_1(|\mathbf{r}_i - \mathbf{r}_j|/\lambda) \hat{\mathbf{r}}_{ij}$ [here $K_1(r/\lambda)$ is a modified Bessel function, λ is the magnetic penetration depth, $\hat{\mathbf{r}}_{ij} = (\mathbf{r}_i - \mathbf{r}_j)/|\mathbf{r}_i - \mathbf{r}_j|$, and $f_0 = \Phi_0^2/8\pi^2\lambda^3$] is the force from the other vortices,⁹ and \vec{F}_i^{vp} is the pinning force. The latter is modeled as $\vec{F}_i^{vp} = -\sum_k^{N_p} M_g R \Phi_0^2 \int_0^\infty dq \frac{1}{Q} J_1(qR) J_1(qr_{ik}) E(q, l, D) / \lambda^2$ (Ref. 10), where $Q = p[p + q \coth(pt/2)]$, $p = \sqrt{1 + q^2}$, $E(q, l, D) = e^{-q l} (e^{-q D} - 1)$, $J_1(x)$ is the Bessel function, t is the thickness of the superconducting film, l is the distance between superconducting film and magnetic dot surface, R and D are, respectively, the radius and thickness of the magnetic dots, r_{ik} is the distance between the vortex i and the mapping center of the magnetic dot on the superconducting film, and $M_g = m/(\pi R^2 D)$ is the magnetization of the dot (m holds for its total magnetic moment) in units of $M_{g0} = \Phi_0/\lambda^2$. This pinning force corresponds to a short-range interaction. It decreases as r_{ik}^{-4} , so that we can use a cutoff assuming that the force is negligible for distances greater than the magnetic dot lattice constant a . To deal with the long range vortex-vortex interaction, \vec{F}_i^{vv} , we have introduced a smoothed method based on a look-up table with steps of 0.04λ up to a distance of 100λ and an interpolation item for distances larger than 100λ (Ref. 11). All the lengths, fields, and forces are given in units of λ , Φ_0/λ^2 , and f_0 , respectively.

In our calculations we first set the parameters of each magnetic dot to the same values as in Ref. 6, except the maximum pinning force, which is taken to be $f_p = 1.117f_0$. Then we consider a 12×12 pinning array with $N_p = 144$ giving a pinning density of $n_p = 4/(9\lambda^2)$ (lattice constant $a = 1.5\lambda$) by fixing the sample with periodic boundary conditions size to $18\lambda \times 18\lambda$ for the AFM and SFM configurations and to $18\lambda \times 18\sqrt{3}/2\lambda$ for the TFM one. The vortices are randomly introduced first and then we anneal the sample from an initial temperature (e.g., critical temperature T_c) to zero. The temperature is reduced to zero in 2500 steps and it remains constant at each step for 1000 molecular dynamic (MD) steps. Once the vortices are stable at zero temperature, we slowly increase the driving force F_d along the horizontal symmetry axis (x axis) of the periodic pinning array from 0 to $1.5f_0$ by $0.001f_0$ every 1000 MD steps, and then we decrease it back to zero at the same speed. We also calculate the velocity and position of each vortex and compute the average velocity in the x direction, $\bar{v}_x = N_v^{-1} \sum_{i=1}^{N_v} \mathbf{v}_i \cdot \hat{\mathbf{x}}$, at every MD step, and write out this average velocity in every 10 MD steps.

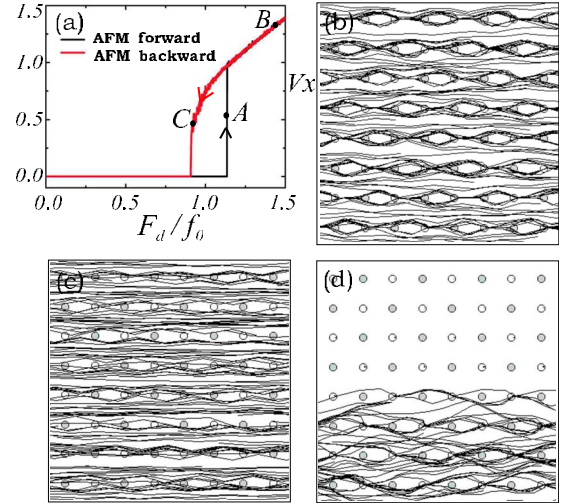


FIG. 1. (Color online) (a) Average vortex velocity versus driving force for a superconducting film with an antiferromagnetic dot array (AFM) with $f_p = 1.117f_0$ at the first matching field [$H/H_1 = 1$, with $H_1 = 2/(9\lambda^2)$]. The driving force F_d is increased from 0 to $1.5f_0$ by $0.001f_0$ and then decreased back to 0. A significant hysteresis with two sharp jumps can be clearly seen at $f_{p,AFM}^{\uparrow} = 1.135f_0$ and $f_{p,AFM}^{\downarrow} = 0.908f_0$. (b) to (d) are the vortex trajectories at the points A, B, and C shown in (a). The black open and gray filled circles in these figures represent, respectively, the up and down-magnetized dots. As it can be seen in (b) and (c), the trajectory lines are topologically stretched along the moving direction with increasing F_d . In the backward branch just before the transition, only part of the vortices are moving while the rest are pinned (d).

III. RESULTS AND DISCUSSIONS

A. AFM configuration

In Fig. 1(a) we present a typical V - I curve of a superconducting film with an AFM magnetic dot array at the first matching field ($H/H_1 = 1$). Since for this configuration only half of the dots are magnetized parallel to the applied magnetic field (“up” direction),⁶ we have chosen $H_1 = 2/(9\lambda^2) = n_p/2$. At the beginning of the forward curve the driving force is too small to overcome the “upper critical force,” $f_{p,AFM}^{\uparrow} = 1.135f_0$, which includes both the attractive force f_p from the local pinning site and the repulsive force from the nearest neighbor (the next antiferromagnetic dot in the moving direction).⁶ Subsequently, all the vortices are pinned and the average velocity in the x direction is zero. At $F_d = f_{p,AFM}^{\uparrow}$, an *almost perfect* first-order transition appears in the V - I curve, as all the vortices are suddenly depinned and either spindly move along the pinning site rows or wavily flow along the channels between two adjacent pinning site rows [Fig. 1(b)]. This first-order transition can be explained as follows: in such a stress overshooting driven system the local avalanche is infinite,⁷ and thus, when any of the vortices is depinned, all the other vortices may respond to it by a simultaneous depinning, leading to a finite jump of the \bar{v}_x . On the other hand, when the vortices are all depinned just outside their pinning sites, as we know, the force F^{vp} is, approximately, inversely proportional to r^4 , which causes a rapid increase in the *total* force acting on the vortices in x

direction, giving rise to a very fast growth of the \bar{v}_x (Ref. 6). If we further increase the driving force, the fluctuation of spindle and wavy paths in the y direction becomes smaller and some of them are even replaced by 1D ones [Fig. 1(c)], an effect that can be interpreted as transverse pinning.^{12,13} After reaching its maximum at $F_d=1.5f_0$, the driving force is decreased at the same speed as it grows. No transition is observed at $F_d=f_{p,AFM}^{\uparrow}$, as in the presence of stress overshoot it is harder to stop the vortex motion than in its absence. As seen in Fig. 1(d), with a further decrease in F_d the rows of vortices are progressively pinned to the “up” magnetic dots and, thus, the average velocity in the x direction drops quickly. Finally, when F_d reaches the lower critical force $f_{p,AFM}^{\downarrow}=0.908f_0$, another “first-order” transition occurs and all the vortices are pinned again. Once the overall motion does stop, the overshoot should have less effect as F_d is increased again.

To further characterize the properties of the configuration-induced hysteresis, we first use the London model¹⁰ to compute the upper critical force as $f_{p,AFM}^{\uparrow}=f_p+F^{vp}(a)\approx 1.135f_0$. Then, we analytically estimate the lower critical force $f_{p,AFM}^{\downarrow}$ and hence the hysteresis width by using an infinite-range model.⁷ The stress overshoot plays the most important role in the transition for the AFM configuration, and it mainly depends on the average velocity in the x direction and on the extra vortex-vortex repulsive forces. From Fig. 1(d) we know that the maximum overshoot happens when a vortex sits in the middle position of two consecutive pinning sites along the y direction while another vortex is pinned by the “up” magnetic dot. The repulsive force between these two vortices is $F^{vv}(a/2)\approx 0.857f_0$ along the y direction. In this situation the average velocity in the x direction is $\bar{v}_x=\Sigma F_x/\eta\approx F_d=f_{p,AFM}^{\downarrow}$. In our model the role of the stress overshoot is played by the long-range vortex-vortex interaction; in analogy to Ref. 7 we can estimate its magnitude surpassing its critical value, $\mu\equiv M-M_c$, as $F^{vv}(a/2)/\bar{v}_x$. By solving the equation, $f_{p,AFM}^{\downarrow}=f_{p,AFM}^{\uparrow}-(1+\mu-\sqrt{1+2\mu})$ (Ref. 7), we get $f_{p,AFM}^{\downarrow}\approx 0.876f_0$ and hence a hysteresis width of $0.261f_0$, which are quite close to the simulation results $0.908f_0$ and $0.247f_0$, respectively.

B. SFM configuration

In Fig. 2(a) we present the V - I curve of a superconducting film with a SFM magnetic dot array at the first matching field ($H/H_1=1$). As it can be seen from the figure, the upper critical depinning force is about $f_{p,SFM}^{\uparrow}=1.104f_0$ and the transition is continuous since the depinning of the vortex lattice is phase-locked; i.e., the interactions between vortices cancel each other yielding no extra vortex-vortex force that may introduce in the system the stress overshoot. Thus, if the driving force is decreased back from values slightly above this critical force no hysteresis is observed. However, when the driving force is continuously increased above point P (for instance up to point A) the average velocity is so large that the pinning potentials are not individual but averaged in the direction of motion. In this situation (called pinning potential washboard¹⁴) the vortices move strictly along the x direction [Fig. 2(d)] and they order in a triangular lattice [Fig. 2(b)].

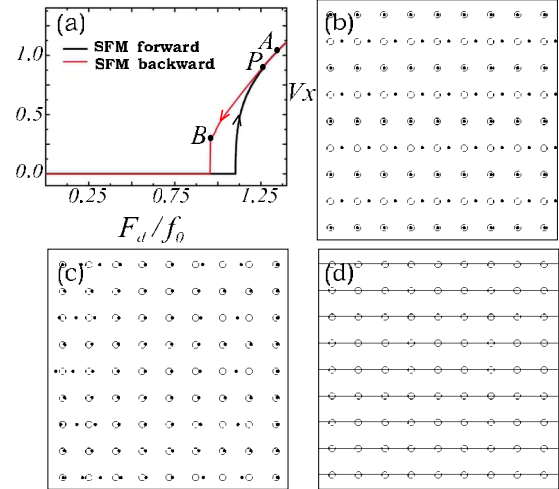


FIG. 2. (Color online) (a) V - I curve for the square ferromagnetic dot array (SFM) configuration at the first matching field ($H/H_1=1$). A significant hysteresis occurs in between $f_{p,AFM}^{\uparrow}=1.104f_0$ and $f_{p,AFM}^{\downarrow}=0.953f_0$. Besides that, the transition from the pinned phase to the moving phase is continuous while the reverse one is discontinuous. (b) and (c) are snapshots of the system corresponding to, respectively, the points A and B in (a), while (d) shows the trajectories of the vortex motion.

Since both the square and triangular vortex lattices are ordered, no extra stress is induced and thus no transition can be observed in the V - I curves when the vortex lattice changes from the square to the triangular one. If we slowly decrease the driving force below point P, the triangular lattice will not return to the square lattice because some vortices are pinned while the others are kept in motion [Fig. 2(c)]. Therefore, extra vortex-vortex interactions are introduced in the system and hysteresis occurs. At $F_d=f_{p,SFM}^{\downarrow}=0.953f_0$, the average velocity is suddenly dropped to zero, which means that all the vortices are pinned at the pinning sites.

We can use again an infinite-range model to analytically estimate the lower critical force. As seen in Fig. 2(c), for the SFM configuration the displacement in a row changes from $+0.5a$ to $-0.5a$ just before the transition of the backward branch. The maximum stress overshoot happens then in a situation where three vortices sit in a row: one is $0.5a$ away from the one in the middle while the other is away in between $0.5a$ and $1.0a$ on the opposite side, choosing $0.75a$ for typification. Therefore, the maximum extra force in the x direction is $\Delta F=F^{vv}(0.5a)-F^{vv}(0.75a)\approx 0.401f_0$, and the magnitude of the stress overshoot surpassing its critical value is $\mu\equiv M-M_c\approx \Delta F/\bar{v}_x=\Delta F/(f_{p,SFM}^{\downarrow}-\Delta F)$. By solving the equation, $f_{p,SFM}^{\downarrow}=f_{p,SFM}^{\uparrow}-(1+\mu-\sqrt{1+2\mu})$, we obtain $f_{p,SFM}^{\downarrow}\approx 0.935f_0$ and thus a hysteresis width of $0.169f_0$, values that are close to the simulation results $0.956f_0$ and $0.148f_0$, respectively.

C. TFM configuration

Finally, in Fig. 3 we present the results obtained by means of the same type of simulations for the TFM configuration. In this case the forward and backward branches perfectly

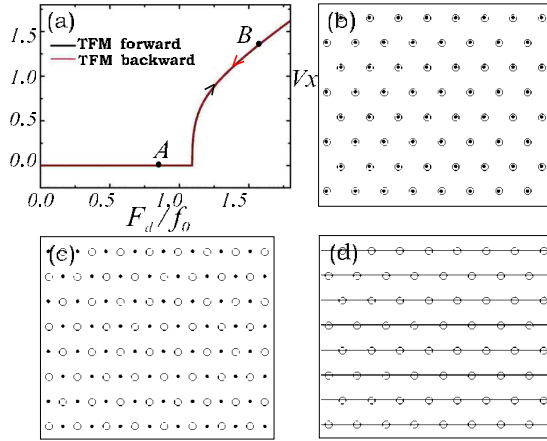


FIG. 3. (Color online) (a) V - I curve for the triangular ferromagnetic dot array (TFM) configuration at the first matching field ($H/H_1=1$). No hysteresis can be observed between the forward and backward branches and the transitions are continuous. (b) and (c) are snapshots of the system corresponding to, respectively, the points A and B in (a), while (d) shows the trajectories of the vortex motion.

overlap and no hysteresis is observed [Fig. 3(a)]. This is because the triangular vortex lattice is the one with the lowest energy, and when the vortex-vortex interaction is strong enough it is difficult to break the symmetry during motion and pinning, even in presence of the pinning potential washboard [Figs. 3(b) and 3(c)]. Therefore, the vortex lattice is always phase-locked and no extra vortex-vortex interactions can be introduced by simply applying a driving force. This explains the absence of the hysteretic behavior for the TFM pinning array.

IV. CONCLUSIONS

To summarize, in the absence of thermal fluctuations the hysteresis and transitions of the voltage-current curves in a superconducting film with PPA at the first matching field are greatly dependent on the configuration of the magnetic dot array. For the AFM configuration, the combination of the vortex-vortex and pin interactions always causes in the system a stress overshoot, giving rise to hysteresis, together with the first-order transitions for both increasing and decreasing driving forces. In contrast, for the SFM configuration no hysteresis occurs and the forward and backward transitions are both continuous provided that the driving force remains below the potential washboard point. If not, hysteresis happens, together with a discontinuous transition in the backward branch. Finally, for the TFM configuration no hysteresis and sharp jumps are observed due to the high stability of the triangular vortex lattice. By using the infinite-range model the lower critical force and the hysteresis width were analytically estimated, and the values are in good agreement with the simulations. Therefore, we conclude that the appearance of the hysteresis along with the first-order transitions and the width of the hysteresis can be controlled by tuning the configuration of the PPA. The physical implications of this unusual hysteretic behavior deserve further studies.

ACKNOWLEDGMENTS

This work was supported by the Research Fund K.U.Leuven under Grant No. GOA/2004/02, BIL China/Flanders, the Belgian Interuniversity Attraction Poles, and the Fund for Scientific Research Flanders (FWO) projects. We also acknowledge support from the NES and AQDJJ-Programmes of the European Science Foundation and from the Ministerio de Educación y Ciencia (Spain) through Grant No. FIS2007-63709. B.Y.Z. also acknowledges the support from the MOST and NSF projects of China.

*qinghua.chen@fys.kuleuven.be

- ¹W. K. Kwok, S. Fleshler, U. Welp, V. M. Vinokur, J. Downey, G. W. Crabtree, and M. M. Miller, *Phys. Rev. Lett.* **69**, 3370 (1992); W. K. Kwok, J. Fendrich, S. Fleshler, U. Welp, J. Downey, and G. W. Crabtree, *ibid.* **72**, 1092 (1994); H. Safar, P. L. Gammel, D. A. Huse, D. J. Bishop, W. C. Lee, J. Giapintzakis, and D. M. Ginsberg, *ibid.* **70**, 3800 (1993); A. E. Koshelev and V. M. Vinokur, *ibid.* **73**, 3580 (1994); B. Y. Zhu, D. Y. Xing, Jinming Dong, and B. R. Zhao, *Physica C* **311**, 140 (1999).
- ²K. Harada, O. Kamimura, H. Kasai, T. Matsuda, A. Tonomura, and V. V. Moshchalkov, *Science* **274**, 1167 (1996); M. Baert, V. V. Metlushko, R. Jonckheere, V. V. Moshchalkov, and Y. Bruynseraede, *Phys. Rev. Lett.* **74**, 3269 (1995).
- ³J. I. Martin, M. Velez, J. Nogues, and Ivan K. Schuller, *Phys. Rev. Lett.* **79**, 1929 (1997); D. J. Morgan and J. B. Ketterson, *ibid.* **80**, 3614 (1998).
- ⁴C. Reichhardt, C. J. Olson, and F. Nori, *Phys. Rev. Lett.* **78**, 2648 (1997); *Phys. Rev. B* **58**, 6534 (1998).
- ⁵B. Y. Zhu, Jinming Dong, and D. Y. Xing, *Phys. Rev. B* **57**, 5063 (1998).
- ⁶Q. H. Chen, G. Teniers, B. B. Jin, and V. V. Moshchalkov, *Phys. Rev. B* **73**, 014506 (2006).
- ⁷J. M. Schwarz and Daniel S. Fisher, *Phys. Rev. Lett.* **87**, 096107

(2001).

- ⁸G. Blatter, M. V. Feigel'man, V. B. Geshkenbein, A. I. Larkin, and V. M. Vinokur, *Rev. Mod. Phys.* **66**, 1125 (1994).
- ⁹J. Pearl, *Appl. Phys. Lett.* **5**, 65 (1964); E. Olive and E. H. Brandt, *Phys. Rev. B* **57**, 13861 (1998).
- ¹⁰M. V. Milošević and F. M. Peeters, *Phys. Rev. B* **68**, 094510 (2003).
- ¹¹Hans Fangohr, Simon J. Cox, and Peter A. J. de Groot, *Phys. Rev. B* **64**, 064505 (2001).
- ¹²U. Yaron, P. L. Gammel, D. A. Huse, R. N. Kleiman, C. S. Oglesby, E. Bucher, B. Batlogg, D. J. Bishop, K. Mortensen, K. Clausen, C. A. Bolle, and F. DeLaCruz, *Phys. Rev. Lett.* **73**, 2748 (1994); F. Pardo, F. DeLaCruz, P. L. Gammel, C. S. Oglesby, E. Bucher, B. Batlogg, and D. J. Bishop, *ibid.* **78**, 4633 (1997); M. Marchevsky, J. Aarts, P. H. Kes, and M. V. Indenbom, *ibid.* **78**, 531 (1997).
- ¹³K. Moon, R. T. Scalettar, and G. T. Zimanyi, *Phys. Rev. Lett.* **77**, 2778 (1996); S. Ryu, M. HELLERQVIST, S. Doniach, A. Kapitulnik, and D. Stroud, *ibid.* **77**, 5114 (1996); C. J. Olson, C. Reichhardt, and F. Nori, *ibid.* **81**, 3757 (1998).
- ¹⁴A. Schmid and W. Hauger, *J. Low Temp. Phys.* **11**, 667 (1973); Gilson Carneiro, *Phys. Rev. B* **66**, 054523 (2002).